Uncertainties of modeling gross primary productivity over Europe: A systematic study on the effects of using different drivers and terrestrial biosphere models

Martin Jung, Mona Vetter, Martin Herold, Galina Churkina, Markus Reichstein, Soenke Zaehle, Philippe Ciais, Nicolas Viovy, Alberte Bondeau, Youmin Chen, et al.

▶ To cite this version:

HAL Id: hal-01788252
https://hal-amu.archives-ouvertes.fr/hal-01788252

Submitted on 17 Sep 2020

Uncertainties of modeling gross primary productivity over Europe: A systematic study on the effects of using different drivers

and terrestrial biosphere models

Martin Jung,[1,2] Mona Vetter,[1] Martin Herold,[3] Galina Churkina,[1] Markus Reichstein,[1] Soenke Zaehle,[4] Philippe Ciais,[4] Nicolas Viovy,[4] Alberte Bondeau,[5] Youmin Chen,[1] Kristina Trusilova,[1,2] Frauke Feser,[6] and Martin Heimann[1]

[1]   Continental to global-scale modeling of the carbon cycle using process-based models is subject to large uncertainties. These uncertainties originate from the model structure and uncertainty in model forcing fields; however, little is known about their relative importance. A thorough understanding and quantification of uncertainties is necessary to correctly interpret carbon cycle simulations and guide further model developments. This study elucidates the effects of different state-of-the-art land cover and meteorological data set options and biosphere models on simulations of gross primary productivity (GPP) over Europe. The analysis is based on (1) three different process-oriented terrestrial biosphere models (Biome-BGC, LPJ, and Orchidee) driven with the same input data and one model (Biome-BGC) driven with (2) two different meteorological data sets (ECMWF and REMO), (3) three different land cover data sets (GLC2000, MODIS, and SYNMAP), and (4) three different spatial resolutions of the land cover (0.25 fractional, 0.25dominant, and 0.5   dominant). We systematically investigate effects on the magnitude, spatial pattern, and interannual variation of GPP. While changing the land cover map or the spatial resolution has only little effect on the model outcomes, changing the meteorological drivers and especially the model results in substantial differences. Uncertainties of the meteorological forcings affect particularly strongly interannual variations of simulated GPP. By decomposing modeled GPP into their biophysical and ecophysiological components (absorbed photosynthetic active radiation (APAR) and radiation use efficiency (RUE), respectively) we show that differences of interannual GPP variations among models result primarily from differences of simulating RUE. Major discrepancies appear to be related to the feedback through the carbon-nitrogen interactions in one model (Biome-BGC) and water stress effects, besides the modeling of croplands. We suggest clarifying the role of nitrogen dynamics in future studies and revisiting currently applied concepts of carbon-water cycle interactions regarding the representation of canopy conductance and soil processes. Citation: Jung, M., et al. (2007), Uncertainties of modeling gross primary productivity over Europe: A systematic study on the effects of using different drivers and terrestrial biosphere models, Global Biogeochem. Cycles, 21, GB4021, doi:10.1029/2006GB002915.

1.   Introduction

[2]   The terrestrial biosphere constitutes a major part of the global carbon cycle and receives large attention in terms of climate change mitigation because of its carbon sequestration potentials [e.g., *Prentice et al.*, 2000]. Within the past decades terrestrial biosphere models (TBMs) have been developed to reproduce and predict carbon stocks and fluxes of the land on continental to global scales [*Cramer et al.*, 2001; *McGuire et al.*, 2001]. TBMs require a range of input (or driving) data, most importantly meteorological, soil and land cover information. Current input data are of heterogeneous nature and origin and modelers need to make

[1]Max Planck Institute for Biogeochemistry, Jena, Germany.
[2]International Max Planck Research School on Earth System Modelling, Hamburg, Germany.
[3]ESA GOFC GOLD Project Office, Department of Geography, Friedrich Schiller University Jena, Jena, Germany.
[4]Laboratory for Climate Sciences and the Environment (LSCE), Joint Unit of CEA-CNRS, Gif-sur-Yvette, France.
[5]Potsdam Institute for Climate Impact Research (PIK), Potsdam, Germany.
[6]GKSS-Forschungszentrum Geesthacht GmbH, Geesthacht, Germany

a choice between alternative driver data sets. The quality of these inputs will have an effect on the accuracy of carbon budget calculations. However, the extent of the effects has not yet been quantified systematically. It is further recognized that uncertainties of TBMs themselves are still rather large, both in terms of parameter-based [e.g., Zaehle et al., 2005], and model structure related uncertainty [e.g., Kramer et al., 2002; Morales et al., 2005; Moorcroft, 2006]. To develop robust estimates of the behaviour of the biosphere in the future, a thorough understanding of input data effects and model uncertainties should lead to a critical review of current modeling performances and avenues to improve known limitations.

[3] Changing the model inputs or changing the model itself means changing the results, but the question is, by how much and in which dimension? Previous studies had looked at individual aspects such as how the spatial resolution, the choice of the meteorological data set, or param-eter uncertainty influences carbon flux simulations, concentrating primarily on net primary production (NPP)[Hicke, 2005; Kimball et al., 1999; Knorr and Heimann, 2001; Turner et al., 2000; Zaehle et al., 2005; Zhao et al., 2006]. The studies differed in the scale from regional to global, and in the way they quantified the effects while generally ignoring effects on spatial and temporal patterns. No systematic study has yet been done that allows us to judge how different options in the model setup affects the magnitude, spatial, and temporal patterns of carbon flux simulations. It is of key importance to elucidate what really matters, i.e., to identify first- and second-order factors. Such knowledge subsequently allows us to improve efficiently our abilities toward accurate estimates of the global carbon budget.

[4] In this paper we present a systematic study that shows how the choice of the model inputs (land cover map, spatial land cover resolution, meteorological data set), and the choice of the process-oriented carbon cycle model itself affect the magnitude, spatial, and temporal patterns of gross primary productivity (GPP) simulations over Europe. We do not aim to identify which data set or model is best but we discuss how these factors constitute limitations on large-scale GPP modeling and how we could improve GPP simulations. GPP is the amount of carbon assimilated by plants via photosynthesis, the process that is believed to be among the best understood within ecosystem carbon cycle modeling. In TBMs, GPP represents the flux how carbon enters the system, and which controls many other processes in the models. If GPP is simulated incorrectly, this error propagates to the other carbon budget variables. GPP is thus a good indicator for the effects of different model setups on simulations of the carbon cycle.

(DGVM) and originates from the BIOME model family [Haxeltine et al., 1996; Kaplan et al., 2003; Prentice et al., 1992]. It simulates the distribution of plant functional types, and cycling of water and carbon on a quasi-daily time step. LPJ has been used in numerous studies on responses and feedbacks of the biosphere in the Earth System [e.g., Brovkin et al., 2004; Lucht et al., 2002; Schaphoff et al., 2006; Sitch et al., 2005]. The version of LPJ used for these calculations has been adapted to account for a realistic treatment of croplands using a crop functional type approach [Bondeau et al., 2007].

[6] The Orchidee DGVM [Krinner et al., 2005] is used as the land surface scheme of the French earth system model IPSL-CM4. It evolved through the unification of the soil vegetation atmosphere transfer model SECHIBA [de Rosnay and Polcher, 1998; Ducoudre et al., 1993] and the terrestrial carbon model STOMATE [Viovy, 1997; Friedlingstein et al., 1998]. The biophysical processes' (photosynthesis and surface energy budget) simulations operate on a half-hourly, and the carbon dynamics simu-lations (allocation, respiration, and aging) on a daily, time step.

[7] Biome-BGC was designed to study biogeochemical processes and has been applied and tested in various studies [e.g., Churkina and Running, 1998; Churkina et al., 2003; Kimball et al., 2000, 1997; Vetter et al., 2005]. It resulted from the generalization of a stand model for coniferous forests (Forest-BGC) [Running, 1994; Running and Gower, 1991] to other vegetation types. It is the only model considered here that includes a nitrogen cycle. As Orchidee, Biome-BGC treats to date croplands as produc-tive grasslands.

2.2. Meteorological and Land Cover Forcings

[8] The requirements of our model intercomparison on meteorological driver data constitute (1) a consistent temporal coverage of several decades, (2) a daily resolution, and (3) an adequately high spatial resolution better than half by half degree. These requirements are met by ERA 40 reanalysis from ECMWF (1961–2000) [European Center for Medium-Range Weather Forecasts (ECMWF), 2000] and simulations by the regional climate model REMO [Jacob and Podzun, 1997; Feser et al., 2001]. REMO was driven by 6-hourly reanalysis from the National Centers for Environmental Prediction (NCEP) [Kalnay et al., 1996; Kistler et al., 2001] from 1948 until 2005 at the boundaries of the European domain. The REMO simulations have a substantially higher spatial resolution (50 by 50 km) than the original T62 NCEP data (approximately 2°) and can be regarded as improved NCEP reanalysis. The REMO data set was chosen to drive all models because it extents until 2005; a prerequisite for a concomitant study on the 2003 heat wave [Vetter et al., 2007].

[9] We chose to use three global 1 km remote sensing based land cover products that became recently available: the MODIS product [Friedl et al., 2002], Global Land Cover 2000 (GLC2000) [Bartholome and Belward, 2005], and SYNMAP [Jung et al., 2006]. SYNMAP has been produced as a synergy of various existing land cover products including GLC2000 and MODIS, and was used

2. Biosphere Models and Driver Data Set Options

2.1. Terrestrial Biosphere Models

[5] We use three state of the art terrestrial carbon cycle models: LPJ [Sitch et al., 2003], Orchidee [Krinner et al., 2005], and Biome-BGC [Running and Hunt, 1993; Thornton, 1998]. LPJ is a dynamic global vegetation model
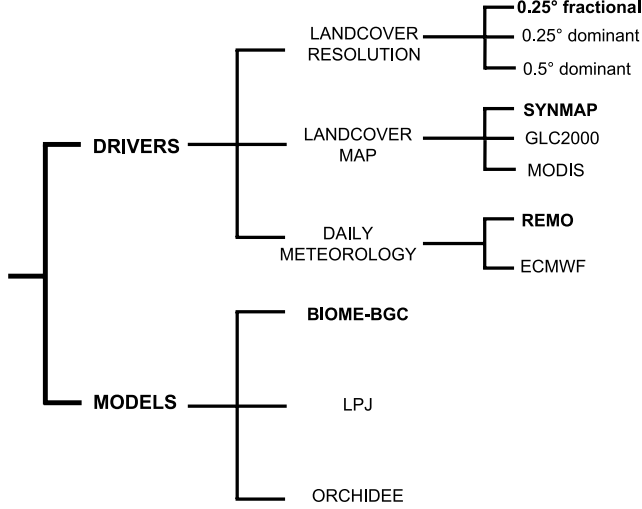
Figure 1. Simulation strategy to assess model performance differences due to the choice of the driver data set and carbon cycle model. Ends of the tree to the right present the different options that we consider. Combination of the reference setup is in bold. From this reference setup only one component is changed at a time within the branch to drive all three models since its plant functional type (PFT) based classification legend meets better the require-ments of biosphere models.[10] We test the effect of prescribing land cover with different spatial detail using a fractional representation of different PFTs within a 0.25 grid cell as well as the dominant PFT with 0.25 and 0.5 spatial resolution.

3. Experimental Design

3.1. Modeling Strategy

[11] We adopt a straightforward strategy where we define a reference setup which consists of the following combination: The model Biome-BGC is forced with the REMO meteorology, and SYNMAP land cover with PFT fractions in a 0.25□ grid cell. Subsequently, we change one of the components at a time: either the model, or the meteorological data set, or the land cover data set, or the spatial resolution. We then compare the simulations with the modified setup to the reference one to quantify the effect of the changed component on the magnitude, spatial pattern and temporal variation of GPP.

[12] Figure 1 displays the modeling strategy in more detail. We make the following changes from the reference setup to yield alternative realizations: (1) spatial land cover resolution: 0.25 and 0.5 dominant vegetation type; (2) land cover map: GLC2000 and MODIS; (3) meteorological forcing: ECMWF ERA 40; and the carbon cycle model: LPJ and Orchidee. We do not consider effects due to different soil water holding capacity (WHC) data because of a lack of alternative data sets. Investigating the model's sensitivity to 50% changes of WHC across 12 sites in Europe is the scope of active research. A detailed modeling protocol that con-tains information on regulations of model spin-up and

transient runs as well as other input data which are kept fixed for all runs such as atmospheric CO_2 concentration, soil and elevation data sets is available in the work of Vetter et al. [2007], and from the Web page (http://www.bgc-jena.mpg.de/bgc-systems/projects/ce_i/index.shtml).

3.2. Quantification of Effects

[13] All calculations to estimate effects on flux magnitudes, spatial and temporal patterns are based on a 20-year period from 1981 to 2000. We measure the effect on the magnitude in percent as the mean absolute difference of the pixel-based means relative to the mean of the reference (equation (1)). To quantify the effect on the spatial pattern we use the variance in percent that is not explained by the squared spatial correlation coefficient between the temporal means of the reference and the alternative realization (equation (2)). We measure the effect on the interannual variability by the variance in percent that is not explained by the squared temporal correlations for each grid cell (equation (3)). The mean effect on the temporal patterns is then calculated as the average over all grid cells.

$$EFFECT_{Magnitude} = \frac{\sum_{i=1}^{n} \left| \overline{AR_i} - \overline{REF_i} \right|}{\sum_{i=1}^{n} \overline{REF_i}} \times 100 \qquad (1)$$

$$EFFECT_{Spatial} = 100$$
$$- \left(\frac{\sum_{i=1}^{n} \left(\overline{AR_i} - \overline{\overline{AR}} \right) \left(\overline{REF_i} - \overline{\overline{REF}} \right)}{\sqrt{\sum_{i=1}^{n} \left(\overline{AR_i} - \overline{\overline{AR}} \right)^2 \times \sum_{i=1}^{n} \left(\overline{REF_i} - \overline{\overline{REF}} \right)^2}} \right)^2$$
$$\times 100 \qquad (2)$$

$$EFFECT_{Temporal}(i)$$
$$= 100 - \left(\frac{\sum_{y=1981}^{2000} \left(AR_y - \overline{AR_i} \right) \left(REF_y - \overline{REF_i} \right)}{\sqrt{\sum_{y=1981}^{2000} \left(AR_y - \overline{AR_i} \right)^2 \times \sum_{y=1981}^{2000} \left(REF_y - \overline{REF_i} \right)^2}} \right)^2$$
$$\times 100 \qquad (3)$$

where i is grid cell index, n is number of valid grid cells, y is year, REF is reference modeling setup, and AR is alternative realization where one component of the reference setup was changed. The single overbar denotes the grid cell based temporal mean. Two overbars denote the mean over all grid cells of the temporal mean.

3.3. Decomposing GPP Into Absorbed Photosynthetic Active Radiation and Radiation Use Efficiency

[14] In order to gain a better understanding of different GPP simulations by different models we decompose GPP

Table 1. Total Gross Primary Product (GPP) of European Domain as Simulated by Different Model Setups (1981–2000 Mean)

Model Setup	GPP of European Domain, GtC/a	Difference From Reference Setup, GtC/a	Difference From Reference Setup, %
Biome-BGC + REMO + SYNMAP + 0.25° fractional	6.181	-	-
Biome-BGC + REMO + MODIS + 0.25° fractional	6.191	0.010	0.2
Biome-BGC + REMO + GLC2000 + 0.25° fractional	5.931	−0.250	−4.0
Biome-BGC + REMO + SYNMAP + 0.25° dominant	6.551	0.370	6
Biome-BGC + REMO + SYNMAP + 0.5° dominant	6.480	0.299	4.8
Biome-BGC + ECMWF + SYNMAP + 0.25° fractional	7.397	1.216	19.7
LPJ + REMO + SYNMAP + 0.25° fractional	7.031	0.851	13.8
Orchidee + REMO + SYNMAP + 0.25° fractional	8.233	2.052	33.2

into absorbed photosynthetic active radiation (APAR) and radiation use efficiency (RUE):

$$GPP = APAR \times RUE \qquad (4)$$

[15] The decomposition is carried out for the simulations by different models individually and follows a standard method that has been applied in previous studies [e.g., Bondeau et al., 1999; Ruimy et al., 1999]. APAR is calculated from fraction of absorbed photosynthetic active radiation (fPAR) and photosynthetic active radiation (PAR) on the basis of monthly data (equation (5)). The fPAR is calculated from modeled LAI according to Lambert-Beer's law assuming a constant light extinction coefficient (k) of 0.5 (equation (6)). PAR is assumed to be a constant fraction of 48% of global shortwave radiation as simulated by REMO (equation (7)). Since we do not account for leaf clumping within the canopy, use constant k and PAR fraction, the derived APAR and RUE values can only be regarded as approximations. However, since we use a consistent methodology the calculated APAR and RUE values are valid for comparison among model simulations.

$$APAR = \sum_{m=1}^{12} fPAR(m) \times PAR(m) \times days(m) \qquad (5)$$

$$fPAR(m) = 1 - e^{-k \times LAI(m)} \qquad (6)$$

$$PAR(m) = 0.48 \times GRAD(m) \qquad (7)$$

where m is month, fPAR is mean fraction of absorbed photosynthetic active radiation, PAR (MJ/m^2) is mean photosynthetic active radiation, days is number of days of month m, LAI (m^2/m^2) is mean (modeled) leaf area index, k is light extinction coefficient (0.5), and GRAD (MJ/m^2) is global (shortwave) radiation.

3.4. Investigating the Models' Response to Meteorology

[16] Differences of model behaviour in terms of interannual variability point to different sensitivities to meteorological conditions. Elucidating the sensitivity of simulated GPP to different meteorological variables is difficult since meteorological variables usually covary strongly, which precludes straightforward separation of the individual effects. We use a principal component analysis (PCA) to effectively reduce the dimensionality of the meteorological input data. We regress the derived variable (first principal component) with simulated variations of GPP to investigate relationship and sensitivity of the models to the meteorol-ogy. To better relate the model's response to meteorological conditions we do not use annual data but data from the summer season (June, July, and August (JJA)). We first compute mean JJA values for each grid cell and year for temperature, radiation, VPD and precipitation. Subsequent-ly, we remove the variable specific mean and perform a z-score transformation of the data before we compute the PCA in IDL 6.3. The new principal components are then regressed with "relative" variations of GPP for each grid cell and model. Relative variations are calculated by first subtracting the grid cell based mean and then dividing by the grid cell based mean. We use relative variations because variability generally scales with the flux magnitude, which differs among models. For all grid cells, we calculate Pearson's correlation coefficient, which gives the strength and direction of the relationship between meteorological and GPP variability, as well as the slope of the linear regression line which provides information on the strength of the response, i.e., sensitivity.

4. Results and Discussion

4.1. Order of Effects

[17] Table 1 summarizes the difference of total GPP of Europe due to alternative model realizations. Changing the meteorological data and the TBM has the largest effects (1.2, 0.9, and 2.1 Gt/a larger GPP for ECMWF, LPJ, and Orchidee, respectively; the reference (Biome-BGC) being 6.2 Gt/a). The spatial patterns of the difference between reference and alternative realizations are presented in Figure 2. The most pronounced effects are again visible for changing the meteorological driver data and the TBM. Major deviations of the ECMWF scenario appear in central, eastern, and northern Europe where the ECMWF driven realization shows substantially higher GPP. The spatial correlation (R^2) of the ECMWF scenario with the reference is 0.67. Changing the model has an even stronger impact on spatial patterns of simulated GPP. In case of Orchidee the
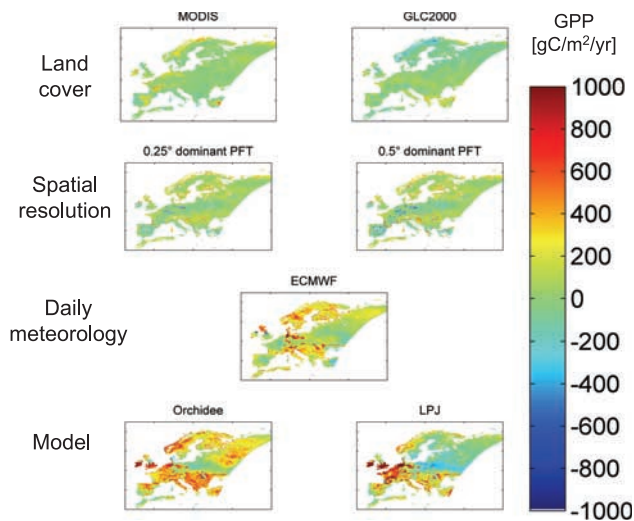
Figure 2. Difference maps of mean European gross primary product (GPP) 1981–2000 for alternative realiza-tions (AR-REF).

correlation (R^2) is 0.54 and for LPJ only 0.2. In the Orchidee simulation the only area where GPP is of similar magnitude is southeast of the Baltic Sea with otherwise higher GPP. The same area shows decreased GPP in the LPJ simulations. The largest differences to the LPJ model are found in western Europe where GPP is up to 1000 gC/m^2/a larger, while small differences are found in northeastern Europe.

[18] Regarding the correspondence of interannual varia-tions of GPP between the reference and alternative realiza-tions we find the same general pattern: poor agreement when changing the meteorological forcing or the model (Figure 3). The ECMWF scenario shows almost no corre-lation of interannual GPP variations with the reference in large parts of eastern Europe and the Mediterranean. When using different models, there are only small areas in north and northeastern Europe where there is moderate to high correlation with the reference. In general the spatial pattern of unexplained temporal variance is similar for the LPJ and Orchidee simulations. This might imply that the Biome-BGC interannual pattern differs substantially from LPJ and Orchidee while the latter two may be similar. When corre-lating the interannual variations of LPJ with Orchidee the large disagreement in temporal variation decreases from on average 60–63% (with LPJ and Orchidee, respectively) to 43% unexplained variance (figure not shown). The correla-tions improve for the boreal region but remain weak over the midlatitude cropland belt and southern Europe (see Figure S1 in the auxiliary material).[1]

[19] Figure 4 summarizes the effects of the different input data sets and models on GPP simulations. There is a clear hierarchy of uncertainties recognizable with a small effect of using different land cover maps, a somewhat higher but still relatively small effect of the spatial land cover resolu-tion, a substantial effect due to changing the meteorological

---

[1]Auxiliary materials are available in the HTML. doi:10.1029/2006GB002915.

---

forcing, and the largest effect caused by using different models. The next sections discuss the individual factors in more detail.

4.2. Land Cover

[20] We note that the land cover data set effect is the smallest one for all investigated scenarios, not reaching 10% on neither magnitude, nor spatial or temporal pattern of modeled GPP. This coincides with findings of Beer [2005] emphasizing the importance of land cover data to be included in carbon modeling but with small effects if different types of existing maps are used. Similar results are reported by Knorr and Heimann [2001] who found a rather small effect of changing the land cover data set on global NPP using the BETHY vegetation model.

[21] Previous studies showed that various land cover classifications derived form remote sensing products have discrepancies among them, particularly in heterogeneous landscapes [Giri et al., 2005; Herold et al., 2006; Jung et al., 2006]. Known global uncertainties for 1 km land cover data sets are in the order of 68% area weighted overall accuracy considering all classes [Mayaux et al., 2006; Scepan, 1999]. However, the map's uncertainty decreases if classes are aggregated to PFTs and the larger grid sizes of the models (here 0.25 fractional). In addition, land cover types derived from satellite data represent direct and con-sistent spatial observations. The other investigated factors involve modeling and thus may contain larger error mar-gins; at least from a theoretical point of view.

[22] While simulations of GPP by TBM seem not to be very sensitive to the land cover map, we expect a much stronger effect on carbon stocks. Deviating cartographic standards and definitions lead to different forest extents and thus carbon stocks. Moreover, our conclusion of small effects of different land cover maps on simulated GPP is restricted to this class of models and data sets, which do not distinguish between crop functional types. To provide a substantial added value of future land cover products the remote sensing community needs to foster the separation of major crop types and management regimes (e.g., irrigated and nonirrigated). Implementing and improving the agricul-tural sector in biosphere models is currently a field of intensive research but partly hampered by the availability of adequate data sets.

4.3. Spatial Resolution of the Land Cover Map

[23] We find the spatial resolution effect on the magnitude of GPP to be 15% and 16% for 0.25° and 0.5° dominant, respectively. In terms of the spatial pattern, only 10% and 14% of the spatial variance remains unexplained. The temporal correlations are only minimal affected (maximum 8% of unexplained variance). The fact that carbon flux calculations are to some extent sensitive to the pixel size have been shown previously and is consistent with this study [e.g., Kimball et al., 1999; Turner et al., 2000]. Turner et al. [2000] used land cover maps of different spatial resolutions (from 25 m to 1000 m) to scale up field measurements from the northwestern United States and found that the difference between 25 m resolution and 1000 m resolution is ~12% for NPP. Kimball et al.
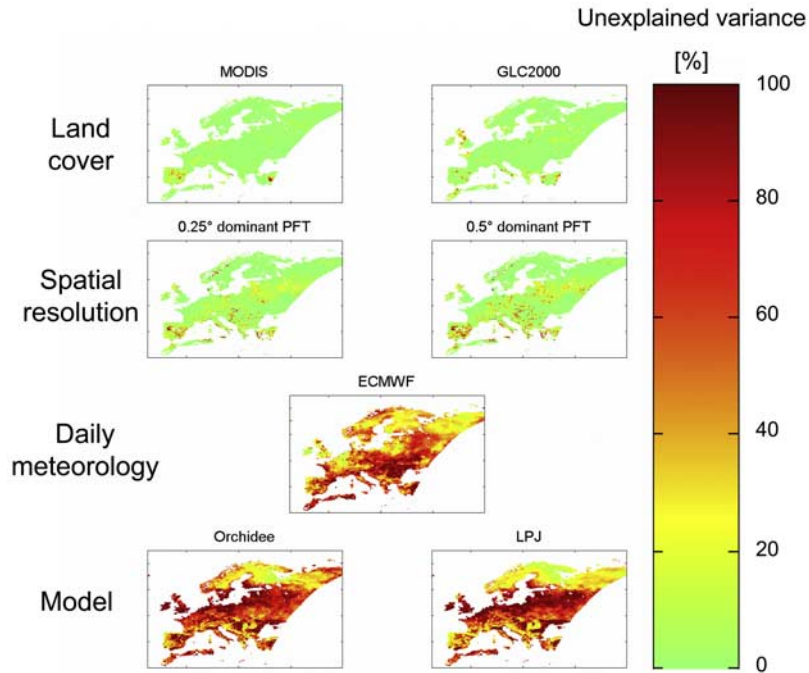
Figure 3. Effect of alternative realizations on the interannual variation of GPP. Fraction of variance that is not explained by the correlation R^2 with the reference setup is shown for each pixel.

[1999] run Biome-BGC with different spatial land cover resolutions over parts of the BOREAS region and found that NPP is affected by 2–14% by spatial aggregation effects.

[24] This study indicates a more prominent effect of changing the spatial resolution compared to changing the land cover data set. It is obvious that a 0.25–0.5 degree cell can only provide a rather coarse representation of the terrestrial vegetation heterogeneity if only the dominant type is mapped. Even the fractional PFT representation from a 1 km resolution land cover map may still introduce representation bias in the carbon budget calculations. Representing vegetation at coarser pixel resolutions often leads to the suppression of certain types that can be important in

terms of carbon cycling. In Europe, for example, this effect applies to the extensive agricultural areas and managed landscapes. Many trees and shrubs along field boundaries, roads, within cities as well as smaller patches of trees can be ''lost'' in pixels that are mapped as, e.g., crop, because this dominates the 1 km mixed pixel. Such bias will soon be reduced by higher-resolution global land cover data sets such as GLOBCOVER.

4.4. Daily Meteorology

[25] The model outputs are more affected by changing the meteorological drivers than for different land cover and spatial resolution options. Total GPP over the European
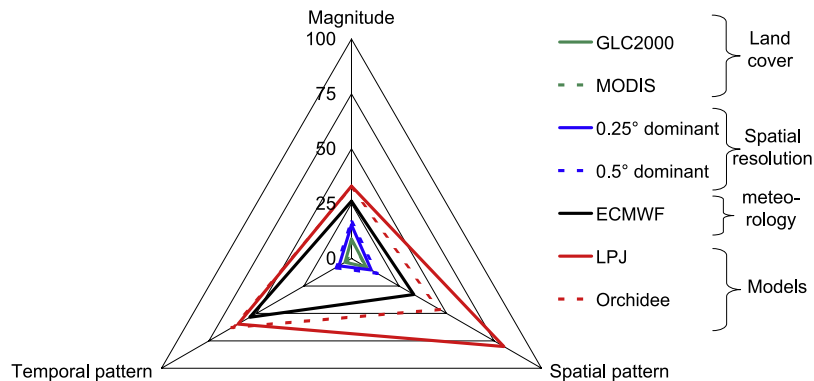
Figure 4. Effects of different model setups (alternative realizations) on the magnitude, spatial, and temporal pattern on GPP simulations over Europe. Measures are in percent and based on the reference period 1981–2000 as explained in section 3.2. No difference to the reference setup would be represented by the center where the axes intersect.

domain of the ECMWF run is 20% higher than the simulations using REMO; the mean absolute difference over all grid cells being 26%. This order of magnitude is comparable to the study of Zhao et al. [2006] on the effect of different meteorological reanalysis (DAO, NCEP, ECMWF) on global GPP and NPP from the diagnostic MOD17 model. In their study, the largest differences occurred between NCEP and ECMWF with ∼23 Gt/a difference for GPP and even higher discrepancies for NPP (∼27 Gt/a). Compared to model runs using meteorological observations, the relative error for GPP ranged from 16% (ECMWF) to 24% (NCEP); for NPP from 45% to 73%. Zhao et al. [2006] concluded that ECMWF appeared to perform best among the reanalysis data sets.

[26] By investigating the differences of mean annual spatial fields of ECMWF and REMO (see Figure S2) we can explain the difference in the spatial patterns of GPP. Northern Europe is warmer and receives more radiation according to ECMWF which results in larger productivity, given that this area is expected to be primarily limited by radiation and temperature. The coinciding higher VPD seems not to counteract this effect suggesting little water limitation over the area in the model. Enhanced gross carbon uptake in southern Europe in the ECMWF runs is related to the higher rainfall in combination with lower VPD since water deficit controls photosynthesis to a large degree here.

[27] We find the interannual variations of GPP due to the different meteorological driver data sets particularly strik-ing. The temporal correlation between REMO and ECMWF radiation data is very weak across almost entire Europe (see Figure S3) and it likely explains the differences in GPP interannual variability over northern Europe where temper-atures are highly correlated. Large discrepancies of interan-nual variations of radiation data sets have also been found by Hicke [2005] who analysed the effect of using different radiation data sets (NCEP, GISS) on global NPP simulations from the CASA model. The author found only a small effect on total global NPP but large effects regarding the spatial pattern and especially interannual variations. For central and eastern Europe the large disagreement of GPP variations between REMO and ECMWF seems to originate from joint effects of differences in radiation, precipitation, and VPD, and likely nonlinear responses due interactions with nitro-gen dynamics in the model (see section 4.5). The temporal correlations of the different data sets for all four meteoro-logical variables are very low for southern Europe and all likely contribute to the deviations in simulated interannual GPP variations.

[28] An in-depth analysis on the differences of the mete-orological data sets and their origins would be insightful but is beyond the scope of this study. Cloud and aerosol physics that govern precipitation and radiation transfer is most likely the major factor that drives the differences among meteo-rological reanalysis. Orographic effects may have further importance; certainly for mountainous regions, which is visible in the difference of mean temperatures (see Figure S2) where REMO temperatures are substantially lower in the mountains because of its finer representation of topography. A detailed comparison and evaluation of

REMO, ECMWF and also other possible meteorological model forcings (NCEP and CRU) is currently in progress [Chen et al., 2007].

[29] Important implications of our findings are that mod-eling studies focusing on interannual variations of carbon fluxes need to consider uncertainties in the meteorological forcing in their interpretations, especially exercises that aim to investigate effects of drought. In addition, it seems crucial to use the same meteorological drivers in model intercom-parison studies. Improved reanalysis would reduce uncer-tainties in the future if long-term consistent time series are provided.

4.5. Biosphere Models

[30] Several model intercomparison studies have shown substantial differences among models [e.g., Cramer et al., 1999; Roxburgh et al., 2004] while mechanistic explana-tions for the differences have been rarely presented. Such task is difficult given that models differ in many respects and isolating the effect of certain alternative parameter-izations is hardly possible given the interactions within the model. We aim to infer the likely most important causes of model differences here to guide future modeling studies, which will allow a more objective judgement on the degree of realism and robustness.

4.5.1. Spatial Patterns

[31] Key factors that likely cause the major differences are related to the model representation of the agricultural sector, nitrogen dynamics, soil hydrology, parameter values, and sensitivity to meteorological conditions, the latter being partly linked to the former factors. LPJ is the only model in this study that has a realistic representation of the agricultural sector. Biome-BGC and Orchidee represent crops as productive natural grassland assuming fertilization (Biome-BGC) or enhanced photosynthetic capacity (Orchidee). The large disagreement among the models in terms of mean annual GPP patterns in the cropland regions is certainly related to this issue (see Figure S4).

[32] Among the three models, nitrogen limitation is only accounted for explicitly in Biome-BGC. This is expected to result in differences among the models along gradients of nitrogen availability such as the transition from boreal to temperate ecosystems. In a recent study we investigated how well the three same models reproduce the spatial gradient of GPP of forest ecosystems across Europe [Jung et al., 2007]. The models appeared to produce a too weak gradient from boreal to temperate forests. We inferred that this resulted primarily from simulating almost no change of LAI, and thus light absorption in the case of LPJ and Orchidee. Biome-BGC performed somewhat better here indicating the effect of increasing nitrogen availability on LAI and light harvesting. GPP is particularly sensitive to the simulated LAI in the range 0 to 3. GPP becomes insensitive to LAI variations when LAI exceeds a value of 4 because changes in light interception become marginal. The signif-icance of the role of nitrogen has also been recently emphasized by Magnani et al. [2007] who suggested that observed relationships between forest GPP and mean annual temperature [e.g., Reichstein et al., 2007] are strongly related to a corresponding gradient of nitrogen availability.
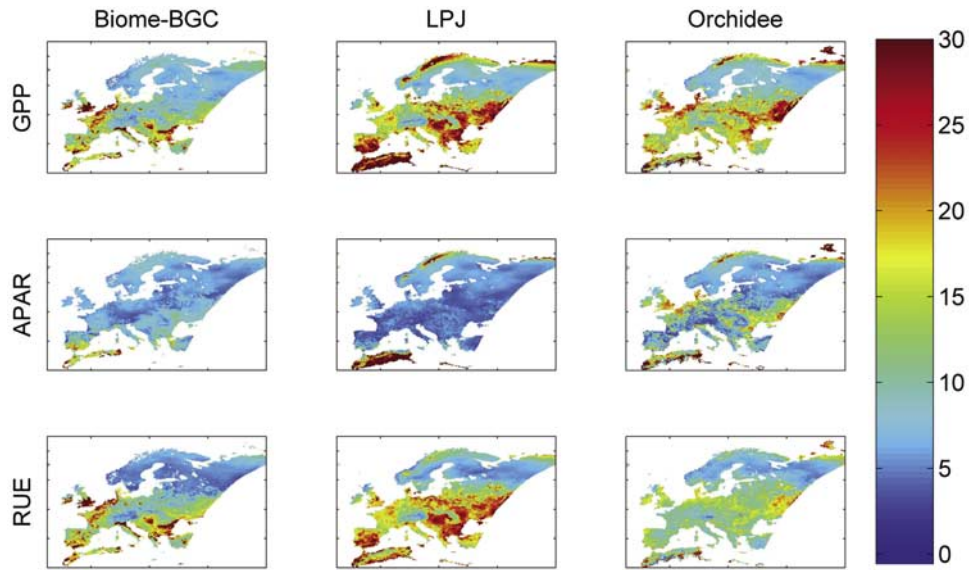
Figure 5. Coefficient of variation (standard deviation divided by mean, in percent) of GPP, absorbed photosynthetic active radiation (APAR), and radiation use efficiency (RUE) for Biome-BGC, LPJ, and Orchidee (1981–2000). Variation of a product (GPP) is predominantly controlled by the factor (APAR or RUE) that shows larger variability. This figure reveals predominant ecophysiological (RUE) control of interannual variability of GPP in the models.

[33] Parameter sensitivity studies [White et al., 2000; Zaehle et al., 2005] have also pointed to the significance of those related to LAI and light absorption such as light extinction coefficient and specific leaf area. Parameters related to maximum photosynthetic capacity and stomata conductance appeared to be at least equally sensitive. A whole series of parameters is associated with PFTs leading to an imprint in the spatial pattern of the simulations according to the PFT distribution while spatial variations within PFTs may be underestimated. Such spatial imprint is visible when one compares the distribution of prescribed vegetation types and simulations of GPP and maximum LAI (see Figure S4). A better understanding of variations and covariations of sensitive parameters in the future may allow removing some of the constraints by fixed parameters and more confidence in predictions. Recent studies link the coordination of plant traits [e.g., Wright et al., 2004] to optimization principles in ecosystems and this approach represents possibly an avenue to overcome some of the limitations [Anten, 2002, 2005; Hikosaka, 2005; Shipley et al., 2006].

4.5.2. Interannual Variability

[34] The low correspondence of simulated interannual variations of Biome-BGC with LPJ and Orchidee is strik-ing. We can gain a first insight into the principal mechanism of GPP variability within the models by decomposing GPP into its "biophysical" and "ecophysiological" component, absorbed photosynthetic active radiation (APAR) and radi-ation use efficiency (RUE), respectively (Figure 5). The spatial pattern of the strength of interannual GPP variation partly differs among models. Biome-BGC and Orchidee show larger variability than LPJ in southern England, the North Sea cost and parts of France while LPJ generates

larger variability on the Iberian peninsular and east of the Adriatic Sea than the other two models. Biome-BGC predicts lower variability north of the Black Sea than LPJ and Orchidee. In general the variation of RUE is stronger then the variation of APAR although differences among models are apparent too. LPJ shows smallest, Biome-BGC intermediate, and Orchidee largest variation of APAR. The relatively higher APAR variability of Biome-BGC and Orchidee result partly from the lower mean maximum LAI (see Figure S4) in the range where fAPAR is sensitive to variations of LAI. In addition carbon allocation operates on a daily time step in Biome-BGC and Orchidee and therefore allows for greater variability of the leaf carbon pool. LPJ in contrast, has annual allocation and leafs are shed only at the end of a season for deciduous vegetation. Variations of fAPAR in the models are somewhat both, cause and consequence of GPP since LAI depends on NPP. Corroboration against APAR data calculated from remotely sensed fAPAR [Gobron et al., 2006] suggests that the variation of APAR may be overestimated by Orchidee in the case of crops and broadleaf trees, by Biome-BGC in the case of broadleaf trees while LPJ may produce too little APAR variability in general (see Figure S5). However, given that RUE varies more and its variations are more strongly correlated with the variations of GPP (see Figure S6) reveals a dominant ecophysiological control of GPP interannual variability in the models. This is consistent with ongoing studies from M. Reichstein (unpublished man-uscript, 2007) for forest ecosystems in Europe. GPP and RUE variations as well as their differences among models are predominant in the middle and low latitudes of Europe suggesting that model differences may result primarily from water stress effects. Since RUE lumps a number of different

Table 2. Result of the Principal Component Analysis (PCA) of the Meteorological Input Data[a]

Principal Component Axis	Variance Explained, %	Eigenvectors			
		Radiation	Temperature	VPD	Precipitation
PCA1	84	−0.283	−0.280	−0.283	0.241
PCA2	11	−0.239	−0.597	−0.311	−1.340
PCA3	3	2.151	−0.234	−1.798	0.137
PCA4	2	1.337	−2.889	2.020	0.581

The PCA was performed on z-score standardized mean data from June to August for each year (mean removed). The eigenvectors give the contribution of the meteorological variables to the different principal component axis model components as well as their interactions into a single number we further investigate the relationship and sensitivity of modeled GPP to meteorological conditions.

[35] The first principal component (PCA1) explains 84% of the variation of the meteorological data set (Table 2). The different meteorological variables contribute to roughly the same amount to this axis as can be seen from the eigen-vectors; negative values are associated with high radiation, temperature, and VPD but low rainfall, positive values the opposite. PCA1 represents a typical weather gradient from ''warm, sunny, and dry'' to "cool, cloudy, and moist''. The three models show strong negative correlations with PCA1 over northern Europe; that is, summer GPP increases correlate with temperature and radiation increases (Figure 6). The sensitivity of the models, expressed as the slope of the regression line, is similar and relatively small as is the GPP variability over this area from the models (see Figure 5).

[36] For the middle and low latitudes of Europe, the relationship reverses; that is, simulated GPP correlates positively with rainfall and negatively with radiation, tem-perature, and VPD. Variations of moisture appear to drive variations of GPP here. The transition from temperature and radiation control to moisture control of GPP is slightly

further south in Biome-BGC. LPJ and Orchidee have similar spatial correlation patterns with PCA1, showing a ubiquitous relationship with moisture while the relationship is stronger for LPJ. Interestingly, Biome-BGC shows no relationship with PCA1 in large parts of the European midlatitudes, particularly in the maritime parts of western Europe. Photosynthesis in Biome-BGC does apparently not always respond to moisture variations in summer. This effect originates most likely from interactions with the nitrogen cycle in Biome-BGC. In years when meteorolog-ical conditions would allow high levels of productivity this level cannot be reached because the nitrogen demand exceeds the supply. Biome-BGC calculates the nitrogen demand on the basis of predefined C:N ratios of different structural compartments of the vegetation, and if the supply is insufficient, the amount of carbon assimilated is corrected down to the level where it matches the nitrogen supply. Productivity, leaf turnover and decomposition, being itself controlled by temperature, soil moisture and nitrogen, determine nitrogen supply. In accordance to our findings, Kirschbaum et al. [2003] have shown that the feedbacks between the carbon and nitrogen cycle in the CenW model have substantial impact on interannual variations of NPP and NEP in Australia. The interactions of carbon and nitrogen dynamics can lead to complex patterns that are often not simply related to meteorological conditions of a growing season. We can partly attribute the substantial disagreement of the interannual variations of GPP between Biome-BGC with LPJ and Orchidee to interactions with nitrogen in Biome-BGC. This feedback between above ground productivity and decomposition in the soil deserves further attention in the future since it has a large effect in the model that includes a nitrogen cycle. For natural ecosys-tems, Anten [2005] and Hikosaka [2005] have shown that interactions with the nitrogen cycle shape ecosystem traits that control photosynthesis assuming optimization princi-pals in ecosystems. Such approach may further be consid-
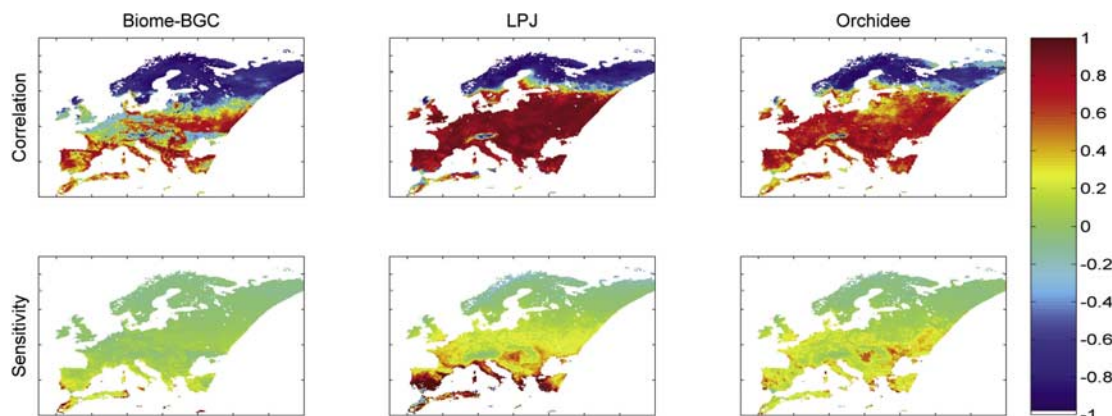
Figure 6. Correlation and sensitivity (slope of regression line) of relative GPP variations to the first principal component of mean JJA meteorology. Negative correlations mean that GPP increases with temperature, radiation, and VPD and decreases with rainfall (northern Europe); positive correlations mean the opposite (central and southern Europe). This shows that the relationship between summer meteorology and simulated GPP is partly different for Biome-BGC and that the three models differ in their sensitivity to meteorological conditions.

ered in the context of global modeling aiming to predict, rather than prescribe, sensitive ecosystem properties.

[37] The sensitivity of the different models to moisture variations is substantially different. Biome-BGC shows least sensitivity and LPJ greatest sensitivity (Figure 6). Orchidee displays only slightly larger sensitivity than LPJ in parts of eastern Europe. Several structural model compo-nents play particularly important roles in determining the response to variations of moisture: (1) interactions with the nitrogen cycle in the case of Biome-BGC as discussed above, (2) the representation of the soil environment, (3) canopy conductance and its feedback to photosynthesis and soil moisture, and (4) direct water stress effects on photo-synthetic capacity.

[38] A smaller sensitivity of Biome-BGC to water stress can be expected given that it represents the soil as a simple one layer bucket without accounting for a differentiated root profile on plant available water. LPJ and Orchidee use two layer models with particular root profiles and depths, depending on the vegetation type. LPJ has a fixed depth of the upper layer of 50 cm while Orchidee's upper layer has dynamic depth, which represents the zone below field capacity. Drying of the upper layer with a higher concen-tration of roots there makes the two models more sensitive to water stress than Biome-BGC, particularly for herba-ceous vegetation with short rooting depths. Orchidee is the only model among the three that uses a parameterization of soil water stress on photosynthetic capacity (Vcmax).

[39] The central linkage between the water and carbon cycle is canopy conductance, which determines intercellular CO_2 concentrations available for photosynthesis and water loss through transpiration, and differences among models in this respect are likely critical. Biome-BGC uses are Jarvis type of approach where a predefined maximum canopy conductance is reduced in a multiplicative scheme of scalars according to environmental conditions (VPD, soil moisture, temperature, radiation, and nitrogen availability). Canopy conductance affects photosynthesis but not the other way round and the feedback comes from the depletion of soil water. In LPJ, canopy conductance, photosynthesis and transpiration are intimately linked. The equations are solved iteratively to yield consistent results according to water demand, and supply from the soil. The strong connection to the soil water status causes downregulation of canopy conductance and photosynthesis as to not fully deplete soil water storage. This mechanism is likely responsible for the strong sensitivity of LPJ to water availability. Orchidee uses the Ball-Berry formulation that relates canopy conductance to assimilation and air humidity and the respective equa-tions are solved iteratively, thus representing a two-way interaction between canopy conductance and assimilation as in LPJ. In contrast to LPJ, canopy conductance in Orchidee is sensitive to air humidity rather than to soil moisture. Differences of sensitivity between LPJ and Orchidee as depicted in Figure 6 may well be related to this factor.

5. Conclusions

[40] We have presented a systematic study on how alter-natives of the model setup affect magnitude, spatial, and temporal patterns of GPP simulations over Europe, using different land cover maps, spatial land cover resolutions, meteorological data sets, and process-oriented TBMs. We found a clear hierarchy of effects: a small effect of using different land cover maps, a somewhat higher but still relatively small effect of the spatial land cover resolution, a substantial effect due to changing the meteorological forcing, and the largest effect caused by using different models.

[41] Differences in the meteorological model forcings affect particularly interannual variations of modeled GPP. Carbon cycle modeling studies that focus on interannual variations need to consider these uncertainties. Furthermore, we strongly recommend using the same meteorological driver data set for each model in intercomparison studies, since otherwise it is not possible to differentiate between model and driver effect when comparing the simulations.

[42] From a model structure point of view, differences between the models in terms of simulating interannual variations of gross carbon uptake are strongly linked to the way of how and if biogeochemical cycles (carbon, water, and nitrogen) interact within the models which controls their sensitivity to meteorological conditions. The related mechanisms used in the models should be clarified and verified since these may shape the carbon cycle climate feedback in Earth system models. We highlight the effect of carbon-nitrogen interactions in altering the effect of inter-annual climate variability on carbon flux variations, here GPP. Water stress effects impact on photosynthesis differ-ently in the models. We suggest revisiting formulations of canopy conductance which represents the central linkages of the carbon and water cycle in the models. In general the representation of soil environment in the models deserves particular attention since processes controlling water and nutrient availability operate here. A sound representation of ecosystem functioning is necessary to capitalize on recent concepts of ecosystem dynamics to changing environmental conditions such as reorganizations of traits to maximize resource use efficiency. Such approaches may lead to more confidence in large-scale modeling, both spatially and temporally, while substantial research still needs to be done in this respect.

References

Anten, N. P. R. (2002), Evolutionary stable leaf area production in plant populations, *J. Theor. Biol.*, *217*(1), 15–32.

Anten, N. P. R. (2005), Optimal photosynthetic characteristics of individual plants in vegetation stands and implications for species coexistence, *Ann. Bot.*, *95*(3), 497–508.

Bartholome, E., and A. S. Belward (2005), GLC2000: A new approach to global land cover mapping from Earth observation data, *Int. J. Remote Sens.*, *26*(9), 1959–1977.

Beer, C. (2005), Climatic causes of the evolution of biomass of Russian forests between 1981 and 1999: An analysis by using a dynamical global vegetation model which is adopted to the boreal zone and constrained by satellite products, Ph. D. dissertation, Friedrich-Schiller-Universitaet, Jena, Germany.

Bondeau, A., D. W. Kicklighter, and J. Kaduk (1999), Comparing global models of terrestrial net primary productivity (NPP): Importance of ve-

getation structure on seasonal NPP estimates, *Global Change Biol.*, *5*, 35–45.

Bondeau, A., et al. (2007), Modelling the role of agriculture for the 20th century global terrestrial carbon balance, *Global Change Biol.*, *13*(3), 679–706.

Brovkin, V., et al. (2004), Role of land cover changes for atmospheric CO_2 increase and climate change during the last 150 years, *Global Change Biol.*, *10*(8), 1253–1266.

Chen, Y., G. Churkina, and M. Heimann (2007), A comparison of regional climate variables between various data sources, *Tech. Rep.*, *8*, 36 pp., Max-Planck-Inst. für Biogeochem., Jena, Germany.

Churkina, G., and S. W. Running (1998), Contrasting climatic controls on the estimated productivity of global terrestrial biomes, *Ecosystems*, *1*(2), 206–215.

Churkina, G., et al. (2003), Analyzing the ecosystem carbon dynamics of four European coniferous forests using a biogeochemistry model, *Ecosystems*, *6*(2), 168–184.

Cramer, W., et al. (1999), Comparing global models of terrestrial net primary productivity (NPP): Overview and key results, *Global Change Biol.*, *5*, 1–15.

Cramer, W., et al. (2001), Global response of terrestrial ecosystem structure and function to CO_2 and climate change: Results from six dynamic global vegetation models, *Global Change Biol.*, *7*(4), 357–373.

de Rosnay, P., and J. Polcher (1998), Modelling root water uptake in a complex land surface scheme coupled to a GCM, *Hydrol. Earth Syst. Sci.*, *2*(2–3), 239–255.

Ducoudre, N. I., K. Laval, and A. Perrier (1993), Sechiba, a new set of parameterizations of the hydrologic exchanges at the land atmosphere interface within the LMD Atmospheric General-Circulation Model, *J. Clim.*, *6*(2), 248–273.

European Center for Medium-Range Weather Forecasts (ECMWF) (2000), ERA-40 project plan, Eur. Cent. for Medium-Range Weather Forecasts, Reading, U.K. (Available at http://www.ecmwf.int/research/era/Project/Plan/Project_plan_TOC.html.)

Feser, F., R. Weisse, and H. von Storch (2001), Multi-decadal atmospheric modeling for Europe yields multi-purpose data, *Eos Trans. AGU*, *82*, 305–310.

Friedl, M. A., et al. (2002), Global land cover mapping from MODIS: Algorithms and early results, *Remote Sens. Environ.*, *83*(1–2), 287–302.

Friedlingstein, P., G. Joel, C. B. Field, and I. Fung (1998), Toward an allocation scheme for global terrestrial carbon models, *Global Change Biol.*, *5*, 755–770.

Giri, C., Z. Zhu, and B. Reed (2005), A comparative analysis of the Global Land Cover 2000 and MODIS land cover data sets, *Remote Sens. Environ.*, *94*, 123–132.

Gobron, N., et al. (2006), Evaluation of fraction of absorbed photosynthetically active radiation products for different canopy radiation transfer regimes: Methodology and results using Joint Research Center products derived from SeaWiFS against ground-based estimations, *J. Geophys. Res.*, *111*, D13110, doi:10.1029/2005JD006511.

Haxeltine, A., I. C. Prentice, and D. L. Creswell (1996), A coupled carbon and water flux model to predict vegetation structure, *J. Vegetation Sci.*, *7*(5), 651–666.

Herold, M., et al. (2006), A joint initiative for harmonization and validation of land cover datasets, *IEEE Trans. Geosci. Remote Sens.*, *44*(7), 1719–1727.

Hicke, J. A. (2005), NCEP and GISS solar radiation data sets available for ecosystem modeling: Description, differences, and impacts on net primary production, *Global Biogeochem. Cycles*, *19*, GB2006, doi:10.1029/2004GB002391.

Hikosaka, K. (2005), Leaf canopy as a dynamic system: Ecophysiology and optimality in leaf turnover, *Ann. Bot.*, *95*(3), 521–533.

Jacob, D., and R. Podzun (1997), Sensitivity studies with the regional climate model REMO, *Meteorol. Atmos. Phys.*, *63*(1–2), 119–129.

Jung, M., K. Henkel, M. Herold, and G. Churkina (2006), Exploiting synergies of global land cover products for carbon cycle modelling, *Remote Sens. Environ.*, *101*(4), 534–553.

Jung, M., et al. (2007), Assessing the ability of three land ecosystem models to simulate gross carbon uptake of forests from boreal to Mediterranean climate in Europe, *Biogeosci. Discuss.*, *4*, 1353–1375.

Kalnay, E., et al. (1996), The NCEP/NCAR 40–year reanalysis project, *Bull. Am. Meteorol. Soc.*, *77*(3), 437–471.

Kaplan, J. O., et al. (2003), Climate change and Arctic ecosystems: 2. Modeling, paleodata-model comparisons, and future projections, *J. Geophys. Res.*, *108*(D19), 8171, doi:10.1029/2002JD002559.

Kimball, J. S., M. A. White, and S. W. Running (1997), BIOME-BGC simulations of stand hydrologic processes for BOREAS, *J. Geophys. Res.*, *102*(D24), 29,043–29,051.

Kimball, J. S., S. W. Running, and S. S. Saatchi (1999), Sensitivity of boreal forest regional water flux and net primary production simulations to sub-grid-scale land cover complexity, *J. Geophys. Res.*, *104*(D22), 27,789–27,801.

Kimball, J. S., A. R. Keyser, S. W. Running, and S. S. Saatchi (2000), Regional assessment of boreal forest productivity using an ecological process model and remote sensing parameter maps, *Tree Physiol.*, *20*(11), 761–775.

Kirschbaum, M. U. F., G. Simioni, B. Medlyn, and R. E. McMurtrie (2003), On the importance of including soil nutrient feedback effects for predicting ecosystem carbon exchange, *Functional Plant Biol.*, *30*, 223–237.

Kistler, R., et al. (2001), The NCEP-NCAR 50–year reanalysis: Monthly means, [CD-ROM and documentation], *Bull. Am. Meteorol. Soc.*, *82*(2), 247–267.

Knorr, W., and M. Heimann (2001), Uncertainties in global terrestrial biosphere modelling: 2. Global constraints for a process-based vegetation model, *Global Biogeochem. Cycles*, *15*(1), 227–246.

Kramer, K., et al. (2002), Evaluation of six process-based forest growth models using eddy-covariance measurements of CO_2 and H_2O fluxes at six forest sites in Europe, *Global Change Biol.*, *8*(3), 213–230.

Krinner, G., N. Viovy, N. de Noblet-Ducoudré, J. Ogée, J. Polcher, P. Friedlingstein, P. Ciais, S. Sitch, and I. C. Prentice (2005), A dynamic global vegetation model for studies of the coupled atmosphere-biosphere system, *Global Biogeochem. Cycles*, *19*, GB1015, doi:10.1029/2003GB002199.

Lucht, W., et al. (2002), Climatic control of the high-latitude vegetation greening trend and Pinatubo effect, *Science*, *296*(5573), 1687–1689.

Magnani, F., et al. (2007), The human footprint in the carbon cycle of temperate and boreal forests, *Nature*, *447*(7146), 849–851.

Mayaux, P., et al. (2006), Validation of the global land cover 2000 map, *IEEE Trans. Geosci. Remote. Sens.*, *44*(7), 1728–1739.

McGuire, A. D., et al. (2001), Carbon balance of the terrestrial biosphere in the twentieth century: Analyses of CO_2, climate and land use effects with four process-based ecosystem models, *Global Biogeochem. Cycles*, *15*(1), 183–206.

Moorcroft, P. R. (2006), How close are we to a predictive science of the biosphere?, *Trends Ecol. Evol.*, *21*(7), 400–407.

Morales, P., et al. (2005), Comparing and evaluating process-based ecosystem model predictions of carbon and water fluxes in major European forest biomes, *Global Change Biol.*, *11*(12), 2211–2233.

Prentice, I. C., et al. (1992), A global biome model based on plant physiology and dominance, soil properties and climate, *J. Biogeogr.*, *19*(2), 117–134.

Prentice, I. C., M. Heimann, and S. Sitch (2000), The carbon balance of the terrestrial biosphere: Ecosystem models and atmospheric observations, *Ecol. Appl.*, *10*(6), 1553–1573.

Reichstein, M., et al. (2007), Determinants of terrestrial ecosystem carbon balance inferred from European eddy covariance flux sites, *Geophys. Res. Lett.*, *34*, L01402, doi:10.1029/2006GL027880.

Roxburgh, S. H., et al. (2004), A critical overview of model estimates of net primary productivity for the Australian continent, *Functional Plant Biol.*, *31*(11), 1043–1059.

Ruimy, A., L. Kergoat, and A. Bondeau (1999), Comparing global models of terrestrial net primary productivity (NPP): Analysis of differences in light absorption and light-use efficiency, *Global Change Biol.*, *5*, 56–64.

Running, S. W. (1994), Testing forest-BGC ecosystem process simulations across a climatic gradient in Oregon, *Ecol. Appl.*, *4*(2), 238–247.

Running, S. W., and S. T. Gower (1991), Forest-BGC, a general-model of forest ecosystem processes for regional applications: 2. Dynamic carbon allocation and nitrogen budgets, *Tree Physiol.*, *9*(1–2), 147–160.

Running, S. W., and E. R. J. Hunt (1993), Generalization of a forest ecosystem process model for other biomes, BIOME-BGC, and an application for the global scale, in *Scaling Physiological Processes: Leaf to Globe*, edited by J. R. Ehleringer and C. B. Field, pp. 141–158, Elsevier, New York.

Scepan, J. (1999), Thematic validation of high-resolution global land-cover data sets, *Photogramm. Eng. Remote Sens.*, *65*(9), 1051–1060.

Schaphoff, S., et al. (2006), Terrestrial biosphere carbon storage under alternative climate projections, *Clim. Change*, *74*(1–3), 97–122.

Shipley, B., M. J. Lechowiecz, I. Wright, and P. B. Reich (2006), Fundamental trade-offs generating the worldwide leaf economics spectrum, *Ecology*, *87*(3), 535–541.

Sitch, S., et al. (2003), Evaluation of ecosystem dynamics, plant geography and terrestrial carbon cycling in the LPJ dynamic global vegetation model, *Global Change Biol.*, *9*(2), 161–185.

Sitch, S., V. Brovkin, W. von Bloh, D. van Vuuren, B. Eickhout, and A. Ganopolski (2005), Impacts of future land cover changes on atmo-

spheric CO_2 and climate, *Global Biogeochem. Cycles*, *19*, GB2013, doi:10.1029/2004GB002311.

Thornton, P. (1998), Regional ecosystem simulation: Combining surface- and satellite-based observations to study linkages between terrestrial energy and mass budgets, Ph.D. thesis, Univ. of Montana, Missoula.

Turner, D. P., W. B. Cohen, and R. E. Kennedy (2000), Alternative spatial resolutions and estimation of carbon flux over a managed forest landscape in western Oregon, *Landscape Ecol.*, *15*(5), 441–452.

Vetter, M., et al. (2005), Partitioning direct and indirect human-induced effects on carbon sequestration of managed coniferous forests using model simulations and forest inventories, *Global Change Biol.*, *11*(5), 810–827.

Vetter, M., et al. (2007), Analyzing the causes and spatial pattern of the European 2003 carbon flux anomaly in Europe using seven models, *Biogeosci. Discuss.*, *4*, 1201–1240.

Viovy, N. (1997), Interannuality and CO_2 sensitivity of the SECHIBA-BGC coupled SVAT-BGC model, *Phys. Chem. Earth*, *21*, 489–497.

White, M. A., P. E. Thornton, S. W. Running, and R. R. Nemani (2000), Parameterization and sensitivity analysis of the BIOME-BGC Terrestrial Ecosystem Model: Net primary production controls, *Earth Interact.*, *4*(3), doi:10.1175/1087-3562 (2000)004<0003:PASAOT>2.0.CO;2.

Wright, I. J., et al. (2004), Leaf trait relationships in Australian plant species, *Functional Plant Biol.*, *31*(5), 551–558.

Zaehle, S., S. Sitch, B. Smith, and F. Hatterman (2005), Effects of parameter uncertainties on the modeling of terrestrial biosphere dynamics, *Global Biogeochem. Cycles*, *19*, GB3020, doi:10.1029/2004GB002395.

Zhao, M., S. W. Running, and R. R. Nemani (2006), Sensitivity of Moderate Resolution Imaging Spectroradiometer (MODIS) terrestrial primary production to the accuracy of meteorological reanalyses, *J. Geophys. Res.*, *111*, G01002, doi:10.1029/2004JG000004.

A. Bondeau, Potsdam Institute for Climate Impact Research (PIK), Telegrafenberg A 31, D-14473 Potsdam, Germany.

Y. Chen, G. Churkina, M. Heimann, M. Jung, M. Reichstein, K. Trusilova, and M. Vetter, Max Planck Institute for Biogeochemistry, Hans-Knöll-Straße 10, D-07745 Jena, Germany. (mjung@bgc-jena.mpg.de)

P. Ciais, N. Viovy, and S. Zaehle, Laboratoire des Sciences du Climat et de l'Environnement (LSCE), Centre Etudes Orme des Merisiers, F-91191 Gif sur Yvette, France.

F. Feser, GKSS-Forschungszentrum Geesthacht GmbH, Max Planck Straße 1, D-21502 Geesthacht, Germany.

M. Herold, ESA GOFC GOLD Project Office, Department of Geography, Friedrich Schiller University Jena, Löbdergraben 32, D-07743 Jena, Germany.